RSC Advances

PAPER

View Article Online
View Journal | View Issue

Cite this: *RSC Adv.*, 2023, **13**, 29768

Sporothioethers: deactivated alkyl citrates from the fungus *Hypomontagnella monticulosa*†

Henrike Heinemann, [a] Kevin Becker, [a] Hedda Schrey, [bc] Haoxuan Zeng, [bc] Marc Stadler [bc] and Russell J. Cox *[a]

Received 23rd August 2023
Accepted 26th September 2023

DOI: 10.1039/d3ra06542a

rsc.li/rsc-advances

Submerged cultivation of *Hypomontagnella monticulosa* MUCL 54604 resulted in formation of a stereoisomeric mixture of new sulfur-containing sporothriolide derivatives named sporothioethers A and B. The presence of the 2-hydroxy-3-mercaptopropanoic acid moiety attenuates the antimicrobial activity in comparison to the precursor sporothriolide suggesting a detoxification mechanism. However, moderate effects on biofilms of *Candida albicans* and *Staphylococcus aureus* were observed for sporothriolide and sporothioethers A and B at concentrations below their MICs.

Alkyl citrates are a structurally broad class of natural products requiring an alkyl citrate synthase (ACS) for their biosynthesis.[1] Examples of fungal alkyl citrates (Scheme 1A) include bysochlamic acid **1**,[2,3] the potent squalene synthase inhibitor squalestatin S1 **2**,[4,5] and piliformic acid **3**.[6] We recently fully characterised the biosynthetic pathway to sporothriolide **8** that is an alkyl citrate isolated from *Hypomontagnella* spp.[7–9] The *spo* biosynthetic gene cluster (BGC) is responsible for production of **8** (Scheme 1B).[10,11] Decanoyl-CoA, produced by a dedicated fatty acid synthase (FAS), is used by the ACS SpoE to form the alkyl citrate **4**. Subsequent enzymatic dehydration to **5**, decarboxylation to **6**, hydroxylation to **7** and lactonization then forms the furofurandione sporothriolide **8** (Scheme 1B). Spontaneous Diels–Alder (DA) reaction with the polyene trienylfuranol A **9**, then results in formation of the sporochartines **10–13** (Scheme 1B). Sporothriolide **8** itself possesses useful antifungal activity.[9] For example it has been shown to protect pepper seedlings from the plant pathogen *Botrytis cinerea*.[12] Sporochartines A-D **10–13**, in turn, are potent cytotoxins active against human cancer cell lines.[11]

Here, we report the isolation, synthesis, structure elucidation, and biological testing of two new sulphur-containing sporothriolide derivatives, termed sporothioether A **14** and B **15** (Fig. 1) from *H. monticulosa* MUCL 54604.[10]

In previous work, sporothriolide **8** was isolated from extracts of *H. monticulosa* MUCL 54604 after cultivation in PDB medium.[10] However, when *H. monticulosa* was cultivated in DPY medium, sporothriolide **8** was not detected. DPY was therefore previously used as a non-producing condition during transcriptomic analysis of the *spo* BGC.[10] However, analysis of the transcriptomic data did not reveal significant down-regulation of the *spo* genes in DPY media, and LCMS analysis of the culture extract revealed the presence of a new metabolite under these conditions. Purification of the new metabolite using preparative reversed-phase chromatography (ESI, Fig. S1†) resulted in isolation of an inseparable 3 : 2 mixture of isomers

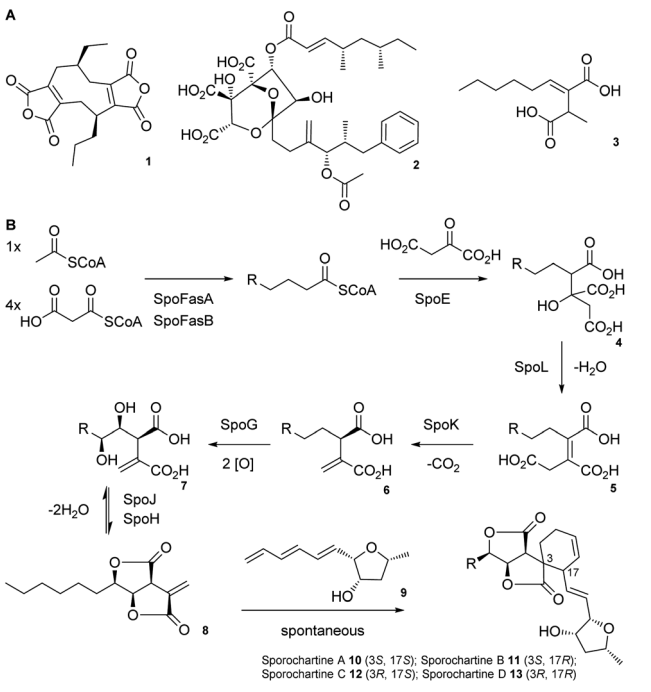

Scheme 1 A) Structures of alkyl citrate metabolites from fungi; (B) biosynthesis of sporothriolide **8** and sporochartines **10–13**. R = C_6H_{14}.

[a]*OCI, BMWZ, Leibniz University of Hannover, Schneiderberg 38, 30167, Hannover, Germany. E-mail: russell.cox@oci.uni-hannover.de*

[b]*Department Microbial Drugs, Helmholtz Centre for Infection Research (HZI), Inhoffenstraße 7, 38124 Braunschweig, Germany*

[c]*Institute of Microbiology, Technische Universität Braunschweig, Spielmannstraße 7, 38106 Braunschweig, Germany*

† Electronic supplementary information (ESI) available. See DOI: https://doi.org/10.1039/d3ra06542a

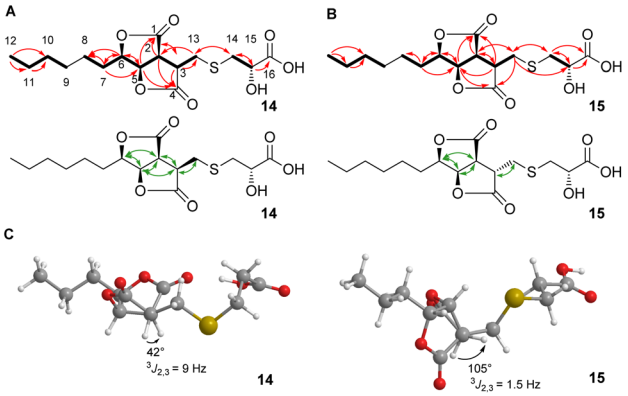

Fig. 1 Key NMR information. (A) COSY correlations (bold lines), HMBC correlations (red arrows) and ROESY correlations (green arrows) of sporothioether **14**; (B) COSY correlations (bold lines), HMBC correlations (red arrows) and ROESY correlations (green arrows) of sporothioether **15**; (C) energy-minimized model structures of sporothioethers **14** and **15** used for a *J*-based assignment of relative stereochemistry.

14 and **15** (as indicated by ^{1}H NMR integrals, ESI, Fig. S5†). A measured *m/z* of 361.1316 $[M + H]^+$ (ESI, Fig. S2†) suggested a molecular formula of $C_{16}H_{24}O_7S$ for each compound. Methylation with TMS-diazomethane led to formation of a 3 : 2 mixture of the corresponding methyl esters **16** and **17** (*m/z* 373 $[M - H]^-$), indicating the presence of a carboxyl group in **14** and **15** (ESI, Fig. S3†).

In the ^{1}H-NMR and HSQC spectra of the **14** and **15** mixture (Table S1†) peaks for a methyl group (δ_H 0.93 ppm), seven methylenes (δ_H 1.34, 1.35, 1.41, 1.50, 1.81, 3.00/(3.08; 2.88), 3.06/(3.24; 2.96)), four methines (δ_H 3.66/3.17, 3.84/3.79, 4.63/4.71, 5.14/5.28) and a hydroxymethine (δ_H, 4.36/4.34) were observed. All peaks were doubled in a 3 : 2 ratio. The ^{13}C data revealed two sets of 16 carbons. Three of the 16 carbons of each set are carbonyls (δ_C 176.4/176.3, 174.6/177.5, 176.1/177.0), seven are methylene carbons (δ_C 23.5, 26.3, 29.8, 29.8/34.3, 30.0, 32.7, 38.4/37.1), one is a methyl carbon (δ_C 14.2) and five are methines (δ_C 44.8/45.6, 45.0/47.7, 72.3, 80.4/81.3, 82.5/83.6).

2D NMR spectra (ESI, Fig. S7–S10†) showed the core structures of **14** and **15** to be the sporothriolide scaffold (Fig. 1A and B). In addition to this core structure, both new compounds harbour a 2-hydroxy-3-mercaptopropanoic acid moiety attached to C-13 of the core *via* a thioether bond. This linkage was supported by the HMBC correlation between CH_2-14 and C-13 (Fig. 1A and B). The presence of the thioether was additionally confirmed by the distinctive ^{1}H/^{13}C chemical shifts of C-13 (**14**, δ_H 3.06 and δ_C 29.8; **15**, δ_H 3.24/2.96 and δ_C 34.3) and C-14 (**14**, δ_H 3.0 and δ_C 38.4; **15**, δ_H 3.08/2.98 and δ_C 37.1). However, the stereochemistry at position C-3 differs in sporothioether A **14** and B **15**. ROESY correlations (Fig. 1, A, B) showed that H-3, H-2, H-5 and H-6 are all *syn* in **14**, but in **15** H-3 is *anti* to H-2, H-5 and H-6, as no ROESY correlation is observed. An energy-minimised model structure of the *anti* diastereomer **15** suggested a dihedral angle of 105° for H-3/H-2 consistent with the observed $^3J_{2,3}$ value of 1.5 Hz (Fig. 1C). In contrast, an energy-minimised model of diastereomer **14** has a dihedral angle of 42° consistent with the observed $^3J_{2,3}$ value of 9 Hz (Fig. 1C). Assuming the same absolute stereochemistry at C-2, C-5 and C-6 as in the parent compound sporothriolide **8**, we conclude that in *syn* diastereomer **14**, C-3 is *R*-configured, and in *anti* diastereomer **15**, C-3 is *S*-configured.

In order to determine the configuration of the stereocenter at C-15 we initially attempted to form Mosher's esters of the 15-OH.[13] However, this approach led to inconclusive results due to the complexity of the spectra of the resulting mixed diastereomers. In an alternative strategy, 15*S* and 15*R* sporothioether derivates were chemically synthesized for comparison by NMR spectroscopy (Scheme 2A).

Commercially available oxirane carboxylate enantiomers **18** and **19** were subjected to regioselective ring opening over two steps by treatment with triphenylmethanethiol to give intermediates **20** and **21**, followed by acidic deprotection to give **22** and **23**. Sporothriolide **8** was purified from *H. monticulosa* and reacted under basic conditions with either **22** or **23**. The resulting sporothioethers were purified by reversed-phase chromatography as inseparable mixtures of diastereomers in each case.

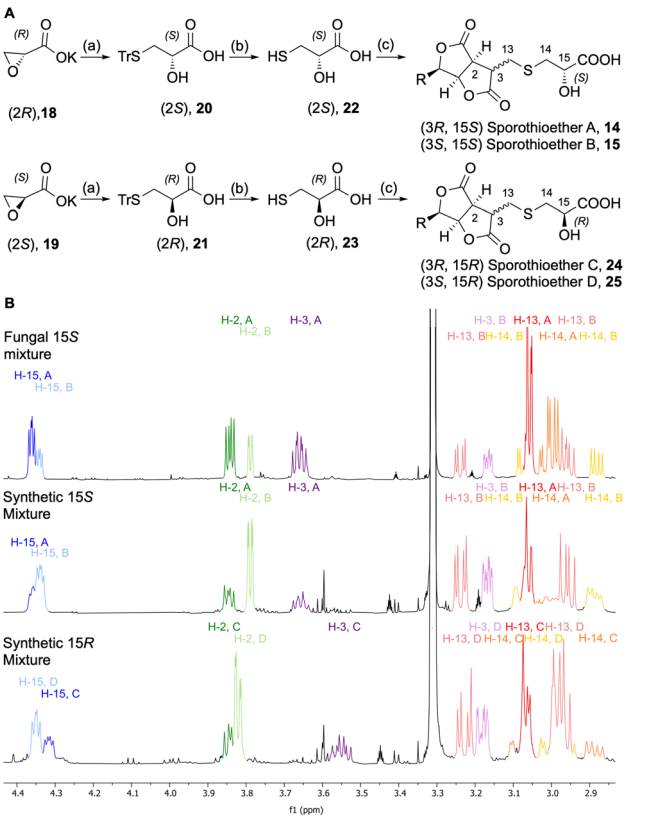

Scheme 2 Synthesis and analysis of sporothioether derivates. (A) Synthetic route towards sporothioethers **14**–**15** and **24**–**25**: (a) TrSH (1.3 eq.), NaH (1.3 eq.), THF, 0 °C-RT, overnight, (b) Et_3SiH (3 eq.), TFA, DCM, 30 min, (c) Sporothriolide **8** (0.8 eq.), Et_3N (5 eq.), CH_2Cl_2, RT, 2 h; Tr = triphenylmethyl; (B) comparison of ^{1}H NMR data of fungal sporothioethers A **14** and B **15**, semisynthetic sporothioether A **14** and B **15** and semisynthetic sporothioether C **24** and D **25**.

Analysis of the ^{1}H NMR data (Scheme 2B) of the synthetic products revealed that both contain a mixture of sporothioether stereoisomers, as indicated by two sets of signals with an integral ratio of 3 : 2. The major compound in both mixtures is 3*S* and the minor component is 3*R*. This was indicated by the $^3J_{2,3}$ value of 1.6 Hz for the 3*S* configured sporothioethers. For the 3*R* configured stereoisomers $^3J_{2,3}$ values of ~9 Hz were observed, the same as for the natural 3*R* sporothioether **14**. ^{1}H NMR chemical shifts of the synthetic (15*S*, 3*RS*)-sporothioether mixture matched the signals of the fungal sporothioether mixture **14** and **15**, whereas the signals of the synthetic (15*R*, 3*RS*)-sporothioether mixture **24** and **25** differed (Scheme 2B). Therefore, sporothioether A **14**, the major compound in the natural mixture, is identified as (3*R*, 15*S*) and the minor compound sporothioether B **15** is identified as (3*S*, 15*S*). The non-natural synthetic diastereomers were now named sporothioether C **24** (3*R*, 15*R*) and sporothioether D **25** (3*S*, 15*R*).

It seems likely that the sporothioethers are biosynthesised by addition of 2*S*-2-hydroxy-3-mercaptopropanoic acid **22** to sporothriolide **8** itself *in vivo*. Formation of an epimeric mixture at C-3 may indicate that this is not an enzymatic process. To test this hypothesis sporothriolide **8** was incubated with 3-mercaptopropionic acid **26** under physiological conditions in phosphate buffer at pH 7.5. LCMS analysis revealed the formation of a new compound with an *m*/*z* of 343 $[M - H]^-$, which corresponds to the mass of the expected product **30** and **31** (ESI, scheme S1†).

The inseparable mixtures of **14** and **15**, and **24** and **25**, were assayed for biological activity (see ESI†). In cytotoxicity assays no activity was detected for the sporothioethers against KB-3-1 and L929 cell lines in the tested range (37–0.63 μg mL^{-1}). Similarly, in previous studies no cytotoxic activity was detected for sporothriolide **8** itself.[9] Both, the sporothioether mixture **14** and **15** and sporothriolide **8**, were tested in biofilm inhibition and dispersion assays against *Stapylococcus aureus* and *Candida albicans* (Table 1). Sporothriolide **8** displayed significant activity against the formation of *S. aureus* biofilms at subtoxic concentrations (MIC (*S. aureus*) > 66.6 μg mL^{-1}), meanwhile only weak inhibitory effects on preformed biofilm of *S. aureus* were observed.

In addition, the sporothioether mixture **14** and **15** displayed moderate inhibitory activity against biofilm formation of *C. albicans* (Table 1). In antimicrobial assays the mixtures of **14** and **15** and **24** and **25** were tested against selected bacteria and fungi in the same assays that were used previously to assess the bioactivity of sporothriolide **8**.[9] The minimum inhibitory concentrations (MIC, Table 2) showed that sporothriolide **8** possesses moderate antimicrobial activity against the tested microorganisms as reported previously,[9] but sporothioethers **14** and **15** were inactive against most organisms and had significantly attenuated effects *vs. Mucor hiemalis* and *Schizosaccharomyces pombe*. Sporothioethers **24** and **25** were inactive against all tested microorganisms.

The sporothioethers **14** and **15** appear to arise by spontaneous addition of 2*S*-2-hydroxy-3-mercaptopropionate to sporothriolide. This is supported by observation of facile addition of 3-mercaptopropionate to **8** in the absence of biological catalysts. This is also consistent with the *S*-configuration of the 2-hydroxy-3-mercaptopropanoic acid moiety in other natural compounds, such as berkeleylactone A **28**,[14] sumularin C **30**,[15] and thiopleurotin **32** (Fig. 2).[16]

For the latter compound, cysteine was identified as the origin for the sidechain **22** and this is also likely to be the case for the sporothioethers.[16,17] In our hands the 3-epimeric forms of the sporothioethers were inseparable. However, it is clear that material isolated from biological and synthetic sources contains differing proportions of the epimers (Scheme 2B). This may be explained by preferential extraction, or preferential degradation, of one epimer from the biological source.

Some of the 2-hydroxy-3-mercaptopropanoic acid moiety-bearing natural compounds have potent bioactivities, whereas others are significantly less toxic in comparison to their originating compounds. For example, sumalarin C **30** is a potent cytotoxin *vs.* tumor cell lines, comparable to its congener 10,11-dehydrocurvularin **29** (Fig. 2).[15,18] Berkeleylactone A **28** displays strong antibacterial effects against Gram-positive bacteria, even though it is denoted as pro-drug of antibiotic A26771B **27**. Here it is hypothesised that the sulfur side chain disrupts the γ-keto-α,β-unsaturated carboxyl, which is thought to be important for bioactivity of the macrolide antibiotic **27** (Fig. 2).[19,20]

In contrast, thiopleurotinic acid A **32**, derived from the cytotoxic and antibacterial compound dihydropleurotinic acid **31** does not possess bioactivity (Fig. 2).[16] Another case in which the addition of 2-hydroxy-3-mercaptopropanoic acid **22** is reported as a detoxification mechanism in fungi is antimicrobial

Table 1 Inhibition of biofilm formation of *Staphylococcus aureus* and *Candida albicans* and dispersion of preformed biofilms of *S. aureus* by sporothioether mixture (**14** and **15**) and sporothriolide **8** at various concentrations; references [%]

Test organism		**14** + **15** mixture	**8**
Biofilm inhibition [% ± SD]	*S. aureus* (DSM 1104)[a]	77 ± 9 (250 μg mL^{-1}) 24 ± 9 (62.5 μg mL^{-1})	75 ± 8 (250 μg mL^{-1}) 55 ± 9 (3.9 μg mL^{-1}) 37 ± 10 (2 μg mL^{-1})
	C. albicans (DSM 11225)[b]	58 ± 8 (250 μg mL^{-1}) 40 ± 10 (31.3 μg mL^{-1})	—
Biofilm dispersion [% ± SD]	*S. aureus* (DSM 1104)[c]	77 ± 9 (250 μg mL^{-1}) 24 ± 9 (62.5 μg mL^{-1})	53 ± 6 (250 μg mL^{-1}) 36 ± 5 (62.5 μg mL^{-1})

[a] Microporenic acid A, 74 ± 12 (250 μg mL^{-1}), 75 ± 6 (7.8 μg mL^{-1}), 42 ± 7 (3.9 μg mL^{-1}). [b] Farnesol: 75 ± 9 (250 μg mL^{-1}), 51 ± 7 (31.3 μg mL^{-1}), 38 ± 10. [c] Microporenic acid A: 64 ± 7 (250 μg mL^{-1}), 41 ± 15 (15.6 μg mL^{-1}); SD: standard deviation; —no inhibition.

Table 2 Minimal inhibitory concentrations (MIC) of sporothioether mixtures (**14** and **15**; **24** and **25**) dissolved in MeOH, sporothriolide **8** and control drugs

	MIC [μg ml^{-1}]			
Test organism	**14** and **15** mix	**24** and **25** mix	**8** (ref. 9)	Ref.
Schizosaccharomyces pombe (DSM 70572)	66.6	—	8.3	4.2[a]
Pichia anomala (DSM 6766)	—	—	33.3	8.3[a]
Mucor hiemalis (DSM 2656)	66.6	—	4.2	4.2[a]
Candida albicans (DSM 1665)	—	—	16.6	8.3[a]
Rhodotorula glutinis (DSM 10134)	—	—	16.6	2.1[a]
Acinetobacter baumannii (DSM 30008)	—	—	nt	0.26[b]
Escherichia coli (DSM 1116)	—	—	—	1.7[c]
Bacillus subtilis (DSM 10)	—	—	—	8.3[c]
Mycobacterium smegmatis (ATCC 700084)	—	—	nt	1.7[d]
Staphylococcus aureus (DSM 346)	—	—	—	1.7[c]
Pseudomonas aeruginosa (PA 14)	—	—	—	0.42[e]
Chromobacterium violaceum (DSM 30191)	—	—	nt	0.42[c]

[a] Nystatin. [b] Ciprobay. [c] Oxytetracyclin hydrochloride. [d] Kanamycin. [e] Gentamycin; – no inhibition; nt, not tested. The cell density was adjusted to 8 × 10^6 cells per ml.

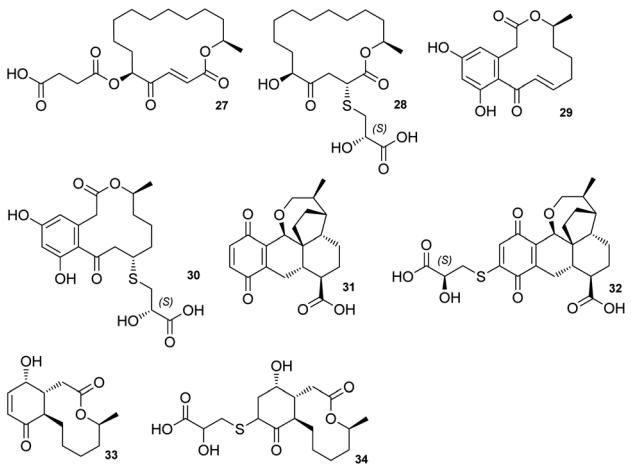

Fig. 2 Structures of metabolites containing the 2-hydroxy-3-mercaptopropanoic acid moiety and their congeners.

compound Sch-642305 **33**. It is converted into a sulfur derivative **34** (Fig. 2) harboring the 2-hydroxy-3-mercaptopropanoic acid moiety in *Aspergillus niger*, losing its bioactivity in the process.[21] Our results are also consistent with the hypothesis that addition of 2-hydroxy-3-mercaptopropanoic acid may be a self-resistance mechanism, as sporothioethers A **14** and B **15** display significantly reduced antifungal activity than the parent compound **8**.

Conflicts of interest

There are no conflicts to declare.

Acknowledgements

This work was funded by the Deutsche Forschungsgemeinschaft priority program "Taxon-Omics: New Approaches for Discovering and Naming Biodiversity" (SPP 1991), specifically CO 1328/4-2 and CO 1328/4-1 and by personal PhD stipend from the "Drug Discovery and Cheminformatics for New Anti-Infectives (iCA)" to HZ, and is financially supported by the Ministry for Science & Culture of the German State of Lower Saxony (MWK no. 21—78904-63-5/19). HH gratefully acknowledges funding from the Leibniz University Hannover. The publication of this article was partially funded by the Open Access Fund of the Leibniz University of Hannover.

Notes and references

1 E. Kuhnert, J. C. Navarro-Muñoz, K. Becker, M. Stadler, J. Collemare and R. J. Cox, *Stud. Mycol.*, 2021, **99**, 1–43.
2 K. Williams, A. J. Szwalbe, N. P. Mulholland, J. L. Vincent, A. M. Bailey, C. L. Willis, T. J. Simpson and R. J. Cox, *Angew. Chem., Int. Ed.*, 2016, **55**, 6784–6788.
3 D. H. R. Barton and J. K. Sutherland, *J. Chem. Soc.*, 1963, 1769–1772.
4 B. Bonsch, V. Belt, C. Bartel, N. Duensing, M. Koziol, C. M. Lazarus, A. M. Bailey, T. J. Simpson and R. J. Cox, *Chem. Commun.*, 2016, **52**, 6777–6780.
5 N. Liu, Y. S. Hung, S. S. Gao, L. Hang, Y. Zou, Y. H. Chooi and Y. Tang, *Org. Lett.*, 2017, **19**, 3560–3563.
6 N. C. J. E. Chesters and D. O'Hagan, *J. Chem. Soc., Perkin Trans.*, 1997, **1**, 827–834.
7 K. Becker and M. Stadler, *J. Antibiot.*, 2021, **74**, 1–23.
8 S. E. Helaly, B. Thongbai and M. Stadler, *Nat. Prod. Rep.*, 2018, **35**, 992–1014.
9 F. Surup, E. Kuhnert, E. Lehmann, S. Heitkämper, K. D. Hyde, J. Fournier and M. Stadler, *Mycology*, 2014, **5**, 110–119.
10 D. S. Tian, E. Kuhnert, J. Ouazzani, D. Wibberg, J. Kalinowski and R. J. Cox, *Chem. Sci.*, 2020, **11**, 12477–12484.
11 C. Leman-Loubière, G. Le Goff, C. Debitus and J. Ouazzani, *Front. Mar. Sci.*, 2017, **4**, 1–9.

12 K. Krohn, K. Ludewig, H. J. Aust, S. Draeger and B. Schulz, *J. Antibiot.*, 1994, **47**, 113–118.
13 T. R. Hoye, C. S. Jeffrey and F. Shao, *Nat. Protoc.*, 2007, **2**, 2451–2458.
14 A. A. Stierle, D. B. Stierle, D. Decato, N. D. Priestley, J. B. Alverson, J. Hoody, K. McGrath and D. Klepacki, *J. Nat. Prod.*, 2017, **80**, 1150–1160.
15 L. H. Meng, X. M. Li, C. T. Lv, C. S. Li, G. M. Xu, C. G. Huang and B. G. Wang, *J. Nat. Prod.*, 2013, **76**, 2145–2149.
16 B. Sandargo, B. Thongbai, M. Stadler and F. Surup, *J. Nat. Prod.*, 2018, **81**, 286–291.
17 B. Ferko, M. Zeman, M. Formica, S. Veselý, J. Doháňošová, J. Moncol, P. Olejníková, D. Berkeš, P. Jakubec, D. J. Dixon and O. Caletková, *J. Org. Chem.*, 2019, **84**, 7159–7165.
18 M. V. De Castro, L. P. Ióca, D. E. Williams, B. Z. Costa, C. M. Mizuno, M. F. C. Santos, K. De Jesus, É. L. F. Ferreira, M. H. R. Seleghim, L. D. Sette, E. R. Pereira Filho, A. G. Ferreira, N. S. Gonçalves, R. A. Santos, R. J. Andersen and R. G. S. Berlinck, *J. Nat. Prod.*, 2016, **79**, 1668–1678.
19 J.-M. Zhang, X. Liu, Q. Wei, C. Ma, D. Li and Y. Zou, *Nat. Commun.*, 2022, **13**, 225.
20 Y. Zhang, J. Bai, L. Zhang, C. Zhang, B. Liu and Y. Hu, *Angew. Chem., Int. Ed.*, 2021, **60**, 6639–6645.
21 E. Adelin, M. T. Martin, M. F. Bricot, S. Cortial, P. Retailleau and J. Ouazzani, *Phytochemistry*, 2012, **84**, 135–140.